

Determination of Rashba-coupling strength for surface two-dimensional electron gas in InAs nanowires

I.A. Kokurin^{1,2,*}

¹*A. F. Ioffe Physical-Technical Institute, Russian Academy of Sciences, 194021 St. Petersburg, Russia*

²*Institute of Physics and Chemistry, Mordovia State University, 430005 Saransk, Russia*

(Dated: March 3, 2024)

A key concept in the field of semiconductor spintronics is an electric field control of spins via the spin-orbit coupling (SOC) and the SOC strength governs efficiency of this control. We propose a new approach that allows the experimental determination of the Rashba SOC strength for ballistic InAs nanowires. The energy spectrum and ballistic transport of carriers through the nanowire with surface two-dimensional electron gas (2DEG) in a homogeneous magnetic field are studied. A general formula for the linear-response one-dimensional ballistic thermopower is derived in the case of complex subband structure. The ballistic conductance and the thermopower are shown to reveal specific features due to strong SOC that allows us to propose a method for the SOC strength determination.

I. INTRODUCTION

Nanowires of narrow gap III-V semiconductors, such as InAs, have recently attracted significant interest in the field of nanoelectronics. InAs nanowire is a good candidate for application in nanodevices such as field effect transistor (FET) [1, 2]. The two-dimensional electron gas (2DEG) is formed close to the surface of an InAs nanowire due to the band bending and the Fermi-level pinning [3] (see Fig. 1a). Thus, a one-dimensional (1D) tubular conducting channel arises near the nanowire surface. Moreover, asymmetric confinement of the surface 2DEG leads to strong Rashba spin-orbit coupling (SOC) [4]. A similar system has been studied theoretically in more complex model [5] where the question of experimental determination of the SOC strength was discussed. A possibility of SOC strength tuning by back or surrounding gate [6] allows to utilize the nanowires in spintronics, e.g. as the basic element of spin-FET proposed by Datta and Das [7] or a gate-defined spin-orbit qubit [8].

Ballistic transport is preferable for spintronic nanodevices but implementation of the ballistic transport regime in InAs nanowires has long hampered due to low carrier mobility that is determined by the surface roughness scattering. However, it was recently demonstrated that the ballistic transport can be realized in short InAs nanowires [2].

Information about the magnitude of spin-splitting and in turn the Rashba SOC strength is important for applications. The antilocalization measurements usually used for experimental determination of Rashba parameter in nanowires [3, 6]. However, such a scheme does not work in the case of ballistic structures. Therefore there is a need to develop a new experimental method to determine the Rashba-coupling strength in ballistic regime.

In present work we study ballistic transport (conductance and thermopower) through the InAs nanowire and propose a method for determining the Rashba SOC strength from transport measurements.

II. MODEL AND SPECTRAL PROBLEM

In order to describe spectral properties of the surface 2DEG in InAs nanowire, we use a simple model of the electron moving on a cylindrical surface of radius r_0 ¹. Note that the surface 2DEG radius r_0 does not coincide with nanowire radius R (see Fig. 1a). For InAs nanowire with $R = 50$ nm the highest electron density is at $r_0 = 42$ nm as was shown in Ref. 9 by means of consistent solution of Poisson and Schrödinger equations. Moreover, applied magnetic field will change the surface 2DEG radius. But in our calculations we suppose the magnetic field to be weak enough and neglect such a dependence.

The Rashba SOC Hamiltonian on the cylindrical surface that was first proposed by Magarill et al. [10] is given by

$$H_{so} = \frac{\alpha}{\hbar}(\sigma_z p_\varphi - \sigma_\varphi p_z), \quad (1)$$

where α is the Rashba SOC parameter, $p_z = -i\hbar\partial/\partial z$, $p_\varphi = -i(\hbar/r_0)\partial/\partial\varphi$, and $\sigma_\varphi = -\sin\varphi\sigma_x + \cos\varphi\sigma_y$ with σ_i ($i = x, y, z$) being the usual Cartesian Pauli matrices. Other authors (see for instance Ref. 11) used SOC Hamiltonian that differs from corresponding one of Ref. 10 in

*Electronic address: kokurinia@math.mrsu.ru

¹ The first radial subband can be taken into account only and the problem could be considered as the effectively quasi-two-dimensional one. It follows from simple estimates that gives about 100 meV for the size-quantization energy (at the well width about 10 nm and the effective mass $0.026m_0$) whereas the Fermi energy is about 150 meV as well as from the strict consistent solution of Poisson and Schrödinger equations [3, 9].

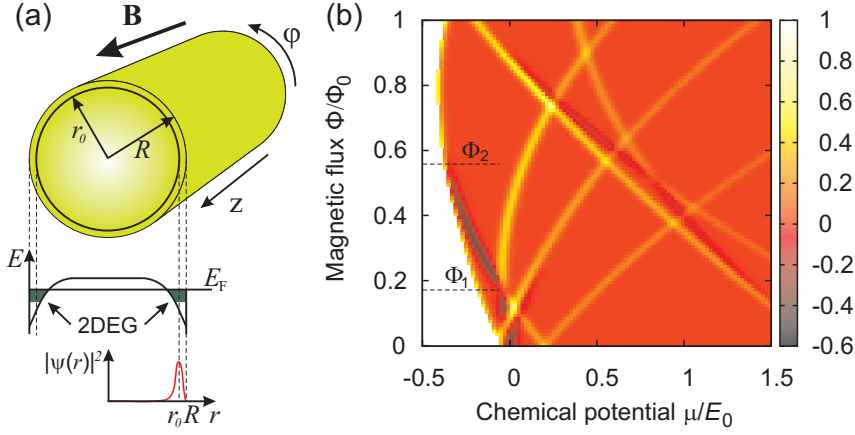


FIG. 1: (Color online) (a) Sketch of the InAs nanowire with radius R placed in homogeneous longitudinal magnetic field. The band bending which leads to surface 2DEG formation is depicted. Carriers are concentrated in thin cylindrical layer of radius r_0 . The radial distribution (squared amplitude of the wave function $|\psi(r)|^2$) is schematically shown. (b) The contour plot of the thermopower S (in units of k_B/e) vs the magnetic flux and the chemical potential, $\Lambda = 0.8$, $T = 0.01E_0$. The specific Φ -values are depicted.

sign². We choose it in such a form because the direction of the normal to 2DEG (in our case it is the inside radial direction) has to coincide with the direction of electric field that leads to the band bending and Rashba-effect [12].

The one-electron Hamiltonian on the cylindrical surface in the presence of Rashba SOC and Zeeman splitting in the uniform longitudinal magnetic field ($\mathbf{B}||z$) is given by

$$H = \frac{\Pi_z^2 + \Pi_\varphi^2}{2m^*} + \frac{\alpha}{\hbar}(\sigma_z \Pi_\varphi - \sigma_\varphi \Pi_z) + \frac{1}{2}g^*\mu_B B \sigma_z, \quad (2)$$

where m^* , g^* , $\mu_B = |e|\hbar/2m_0c$ are effective mass, g-factor and Bohr magneton, respectively, $\mathbf{\Pi} = \mathbf{p} - \frac{e}{c}\mathbf{A}$ is the kinetic momentum with \mathbf{A} being the vector potential of the magnetic field ($A_\varphi = Br_0/2$, $A_z = 0$)³.

Since the Hamiltonian (2) commutes with p_z (translational invariance) and with the operator of z -projection

of total angular momentum $j_z = -i\hbar\partial/\partial\varphi + (\hbar/2)\sigma_z$ (rotational invariance) we will look for the eigenstates in the following form

$$\Psi(\varphi, z) = \frac{e^{ikz}}{\sqrt{2\pi L}} \begin{pmatrix} e^{i(j-1/2)\varphi} C_{jk}^{(m)} \\ e^{i(j+1/2)\varphi} D_{jk}^{(m)} \end{pmatrix}, \quad (3)$$

where L is the nanowire length, $\hbar k$ is the longitudinal momentum, and the spinor components $C_{jk}^{(m)}$ and $D_{jk}^{(m)}$ are in general k -dependent due to SOI.

The solution of Schrödinger equation for the Hamiltonian (2) with the obvious periodicity condition $\Psi(\varphi + 2\pi, z) = \Psi(\varphi, z)$ yields for the energy spectrum

$$\frac{E_{jm}(k)}{E_0} = (kr_0)^2 + (j + \Phi/\Phi_0)^2 + 1/4 - \Lambda/2 + m\sqrt{(\Lambda kr_0)^2 + [\Delta - (1 - \Lambda)(j + \Phi/\Phi_0)]^2}, \quad (4)$$

where $E_0 = \hbar^2/2m^*r_0^2$ is the character energy scale in the problem, $\Lambda = r_0/l_{so}$ is the dimensionless SOC parameter with $l_{so} = \hbar^2/2m^*\alpha$ being the character SOC length, $j = \pm 1/2, \pm 3/2, \dots$ is the z -projection of total angular momentum, $m = \pm 1$ labels two branches of the spin-split energy spectrum, Φ is the magnetic flux $\pi r_0^2 B$ through a section of the surface 2DEG, $\Phi_0 = 2\pi\hbar c/|e|$ is the flux quantum, and $2\Delta = g^*\mu_B B/E_0$ is the dimensionless Zeeman splitting.

The normalized eigenspinors in (3) are given by

$$C_{jk}^{(+)} = D_{jk}^{(-)} = \cos\left(\frac{\theta_{jk}}{2}\right), \quad D_{jk}^{(+)} = C_{jk}^{(-)} = i \sin\left(\frac{\theta_{jk}}{2}\right), \quad (5)$$

where $\tan \theta_{jk} = \Lambda kr_0/[\Delta - (1 - \Lambda)(j + \Phi/\Phi_0)]$.

The energy spectrum and its evolution with magnetic field is depicted in Fig. 2. At zero magnetic field the spectrum (4) corresponds to the result of Ref. 10. The

² In Refs. 10, 11 the model Hamiltonian (1) was considered in other context and the direction of band bending was not exactly taken into account. However, the relationship between the direction of the normal to the cylindrical surface (inside or outside) and the Rashba-coupling sign was discussed [10]. The above inconsistency in sign of Eq. (1) is apparently due to the domination in the literature of the following form of Rashba SOC operator [4], $H_{so} = (\alpha/\hbar)\boldsymbol{\sigma} \times \mathbf{p} \cdot \mathbf{n}$, with \mathbf{n} being the unit vector of the normal to 2DEG (not the unit vector of built-in or external electric field) that, however, does not cause misunderstandings in the case of flat 2DEG-structure.

³ It should be noted the vector potential that enters Eq. (2) is no longer real vector potential and equation $\mathbf{B} = \nabla \times \mathbf{A}$ fails for it. The real vector potential that yields the correct \mathbf{B} is r -dependent and it enters the initial three-dimensional Hamiltonian that has to be averaged over ground state of transverse motion (radial direction) in order to obtain the Hamiltonian with lower dimension.

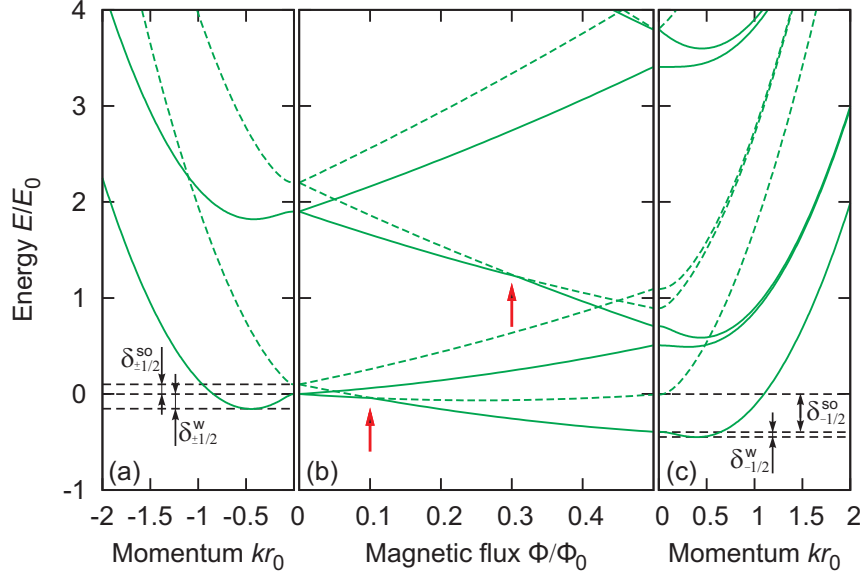


FIG. 2: (Color online) The influence of magnetic flux on energy spectrum of the surface 2DEG, $\Lambda = 0.9$. Full (dashed) lines denote subbands with $m = -1$ ($m = +1$). (a), (c) The subband spectrum: (a) $\Phi = 0$; (c) $\Phi = 0.5\Phi_0$. The magnitudes δ_j^{so} and δ_j^w are depicted for the lowest subbands. (b) The evolution of 1D-subbands with magnetic flux increasing at $k = 0$. Arrows indicate the magnetic flux values at which the subbands $(j, -1)$ and $(j, +1)$ coincide at $k = 0$ (there is no SO-gap).

applied magnetic field lifts the degeneracy on the sign of j . For strong SOC there are W-shape subbands with $m = -1$ (there are two minima and one maximum), which appearance depends on relation between Λ and Φ . The W-like shape exists in $(j, -1)$ -subband if the following condition is fulfilled, $\Lambda^2/2 - |\Delta - (1 - \Lambda)(j + \Phi/\Phi_0)| > 0$.

The so-called spin-orbit (SO) gap [13] occurs in above-mentioned subbands. It is the energy distance between $(j, -1)$ -subband maximum and $(j, +1)$ -subband minimum. The width of SO-gap (in E_0 units) for $(j, m = \pm 1)$ -subbands is

$$\delta_j^{so} = 2|\Delta - (1 - \Lambda)(j + \Phi/\Phi_0)| \quad (6)$$

and can vanish at specific Φ -values (Fig. 2). The observation of SO-gap was experimentally performed in quantum wires that defined in two-dimensional hole gas [13].

The energy distance between the two minima and one maximum in W-shape subband is given by

$$\delta_j^w = \Lambda^2/2 - |\Delta - (1 - \Lambda)(j + \Phi/\Phi_0)| \quad (7)$$

and at specific Φ tends to zero leading to the flat subband shape at $k = 0$. We use these properties below for determination of SOC strength. The magnitudes δ_j^{so} and δ_j^w are depicted in Fig. 2.

The SO-gap can occur even in zero magnetic field unlike the case of planar quantum wires of Ref. 13. It takes place under the following condition, $\Lambda^2 > 2|(1 - \Lambda)j|$. If there is SO-gap then its width varies linearly with the SOC strength. Our estimations show that the W-like subband shape can take place even at $\Lambda \sim 0.05$, but in this case the Φ -range of the W-shape structure existence is very narrow and the energy distance between extrema

δ_j^w is small as well, so that the low temperature about 10 mK smoothes all relating effects. Thus, SOC can be assumed to be strong at $\Lambda \gtrsim 0.5$.

III. BALLISTIC CONDUCTANCE AND THERMOPOWER

Let us consider ballistic transport in the above system. There are some differences between the well-known ballistic transport through the 1D system with a parabolic dispersion and the transport in a system with a complex spectrum. At first, we write the general formulae for finite-temperature ballistic conductance and thermopower (Seebeck coefficient) of the quasi-1D system in the case when subbands have an arbitrary number of extrema.

Now we consider a system that consists of two electron reservoirs with chemical potentials $\mu_{L(R)}$ and temperatures $T_{L(R)}$ (the temperature is in the energy units) connected by a nanowire. We assume the transport through the nanowire to be ballistic, i.e. there is no scattering inside the system and the scattering at the nanowire-reservoir contact region is negligible. Therefore a transmission coefficient $T(E)$ within any subband is energy-independent and equals to unity (i.e. there is the perfect transmission and no mode mixing, $T_{j'm',jm}(E) = \delta_{j'j}\delta_{m'm}$). If dc bias V and temperature difference ΔT are applied between reservoirs, so that $\mu_L = \mu_R - eV$ and $T_L = T_R - \Delta T$ ($\Delta T > 0$), then the net current I is

given by (see for instance Ref. 14)

$$I = \frac{e}{2\pi} \sum_{j,m} \int_{-\infty}^{\infty} dk v_{jmk} [\theta(v_{jmk}) f(E, \mu_L, T_L) + \theta(-v_{jmk}) f(E, \mu_R, T_R)], \quad (8)$$

where $v_{jmk} = \partial E_{jm}(k)/\partial(\hbar k)$ is the (j, m) -subband electron velocity, $\theta(x)$ is the Heaviside unit step function, $f(\varepsilon, \mu, T) = \{1 + \exp[(\varepsilon - \mu)/T]\}^{-1}$ is the Fermi distribution function. Here $\theta(\pm v_{jmk})$ ensures that the contribution to the current is given by electrons moving from the left (right) reservoir to the right (left) one only. It should be noted, that within Landauer-Büttiker transport framework reservoirs enter the transport equations through the chemical potential only (see for instance Refs. 15, 16 and references therein) and there is no influence of energy dispersion in reservoirs on 1D transport.

After transition to E -integration the formula for the net current can be rewritten in the form

$$I = \frac{e}{2\pi\hbar} \sum_{j,m} \left[\int_{\infty}^{E_{jm}^{(1)}} dE f(E, \mu_R, T_R) + \int_{E_{jm}^{(1)}}^{E_{jm}^{(2)}} dE f(E, \mu_L, T_L) + \dots + \int_{E_{jm}^{(N_{jm})}}^{\infty} dE f(E, \mu_L, T_L) \right], \quad (9)$$

where $E_{jm}^{(n)}$ is the energy value at n -th local extremum of (j, m) -subband and total number of extrema in the subband (j, m) is N_{jm} . We have one or three extrema as was discussed earlier.

If applied bias voltage V and temperature difference ΔT are assumed to be low, $\Delta\mu = -eV \ll \mu_{L(R)}$, $\Delta T \ll T_{L(R)}$ (linear-response regime), then the conductance and thermopower

$$G = \left(\frac{eI}{\Delta\mu} \right)_{\Delta T=0}, \quad S = \frac{k_B}{e} \left(\frac{\Delta\mu}{\Delta T} \right)_{I=0} \quad (10)$$

can be found from (9). Here k_B is the Boltzmann constant.

One can obtain from (9), (10) Pershin et al. result for conductance [17]

$$G = \frac{G_0}{2} \sum_{jm} \sum_n \beta_{jm}^{(n)} f(E_{jm}^{(n)}, \mu, T). \quad (11)$$

Here $G_0 = e^2/\pi\hbar$ is the conductance quantum (for spin-degenerate case), and $\beta_{jm}^{(n)} = +1$ if n -th extremum of (j, m) -subband is the minimum point but $\beta_{jm}^{(n)} = -1$ if n -th extremum of (j, m) -subband is the maximum one. The sum in (11) is over all extremal points of all subbands.

For the thermopower S we find from (9) and (10) the following equation

$$S = \frac{k_B}{e} \frac{\sum_{jm} \left[\ln 2 + \sum_n \beta_{jm}^{(n)} F\left(\frac{E_{jm}^{(n)} - \mu}{2T}\right) \right]}{\sum_{jm} \sum_n \beta_{jm}^{(n)} f(E_{jm}^{(n)}, \mu, T)}, \quad (12)$$

where the function $F(x) = \ln(\cosh x) - x \tanh x$ has the following properties: $F(-x) = F(x)$, $F(\pm\infty) = -\ln 2$, and $F(0) = 0$. The function $F[(E - \mu)/2T]$ as a function of the chemical potential μ represents a narrow symmetric peak with a width about several T .

In accordance with Eqs. (11) and (12), positions of conductance up-(down-)steps and thermopower peaks (dips) correspond to coincidence of the chemical potential with the minimum (maximum) in the energy spectrum. The dependencies of G and S on the chemical potential μ , calculated by means of Eqs. (11) and (12), are depicted in Fig. 3. One can see the usual step-like conductance increasing with μ -increasing and regular thermopower oscillations [18, 19] in the case of weak SOC (in this case the 1D-subbands have near-parabolic shape and single minimum is in each subband). Each spin-split subband contributes $+G_0/2$ to the total conductance. In the case of simple subband dispersion one can immediately obtain from (12) the Streda result [18] that determines the thermopower magnitude at the maxima

$$S_i^{\max} = \frac{k_B}{e} \frac{\ln 2}{i + 1/2}, \quad (13)$$

where i is a peak number or a number of occupied subbands. This equation fulfills at low temperatures when thermopower peaks are sufficiently narrow and they do not overlap each other.

In the opposite case of strong SOC specific features appear: conductance down-steps ($-G_0/2$ -steps) and negative thermopower dips. These features correspond to coincidence of the chemical potential with the maximum in 1D-subband. The presence of successive $+G_0$ -step and $-G_0/2$ -step in $G(\mu)$ -dependence is the contribution of W-shape subband. The width of corresponding \sqcap -like plateau is obviously equal to δ_j^w . The SO-gap δ_j^{so} is equal to the corresponding \sqcup -like plateau width in conductance and the distance between sequential dip and peak in thermopower. At strong SOC and $B = 0$ (when SO-gap exists) the dependence $G(\mu)$ will have $+2G_0$, $+G_0$ and $-G_0$ steps due to the two-fold j -degeneracy.

As the temperature increases one can see the smearing of conductance steps, since electrons coming in from reservoirs no longer have a sharp steplike energy distribution. The down-step disappears at the temperature about $\min(\delta_j^{so}, \delta_j^w)$. At the same temperature the corresponding negative thermopower dip vanishes that is due to the overlapping with a neighboring peak. Thus, low temperatures are necessary for the negative thermopower observation.

The applied magnetic field changes a position of subband extrema (and even the number of extrema) and these changes are seen in transport characteristics. A contour plot of the thermopower vs the magnetic flux and the chemical potential is shown in Fig. 1b. This figure will be discussed below in application to the determination of the SOC strength parameter.

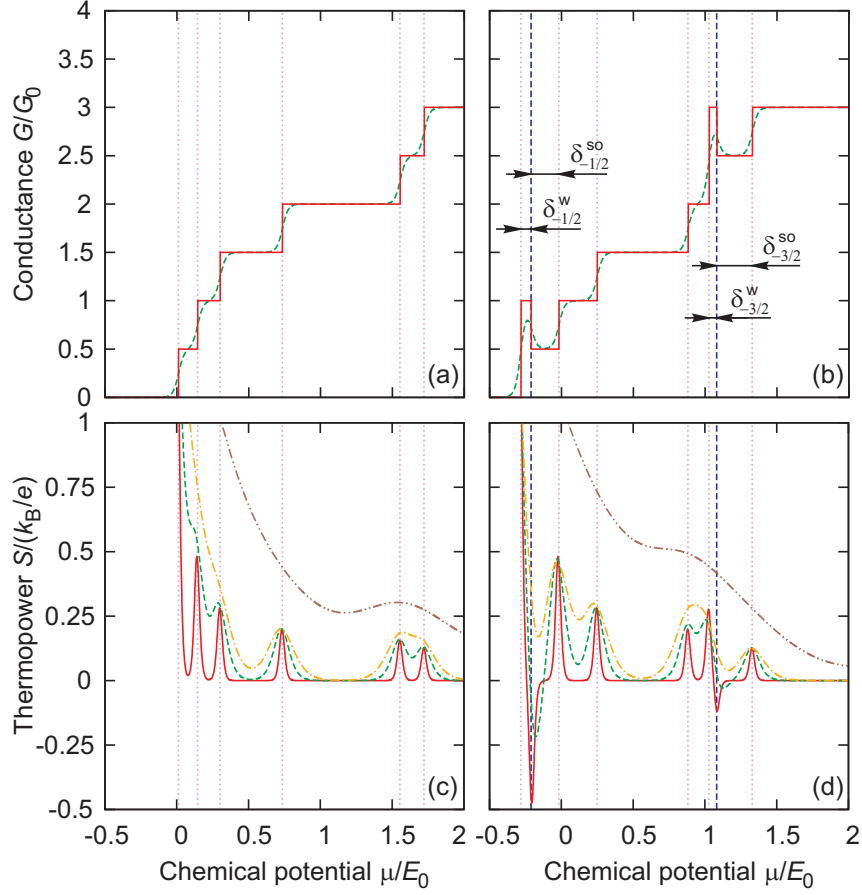


FIG. 3: (Color online) Conductance (a), (b) and thermopower (c), (d) as a function of the chemical potential. (a), (c) Weak SOC, $\Lambda = 0.15$, $\Phi = 0.28\Phi_0$; (b), (d) Strong SOC, $\Lambda = 0.78$, $\Phi = 0.34\Phi_0$; (a), (b) Full line, $T = 0$; dashed line, $T = 0.02E_0$; (c), (d) Full line, $T = 0.01E_0$; dashed line, $T = 0.03E_0$; dot-dashed line, $T = 0.05E_0$; double-dot-dashed line, $T = 0.2E_0$. The vertical dashed (dotted) lines denote the position of the energy maxima (minima). The magnitudes δ_j^{so} and δ_j^w are depicted for the case of strong SOC.

IV. DETERMINATION OF RASHBA-COUPPLING STRENGTH PARAMETER

Now we discuss the approach for determination of the SOC strength parameter α from transport measurements that based on detection of mentioned spectral features evanescence with changing magnetic field. We do not describe any experimental setups here. The principal requirement to experimental setup is the possibility of independent control of Rashba-coupling parameter (that has to be extracted from measurements) and Fermi-level position. Metallic gates or optical excitation can be utilized for the chemical potential tuning.

In Fig. 1b one can see two features: (i) the thermopower peak-dip annihilation ($S = 0$) and (ii) dip disappearance close to the peak of higher amplitude ($S > 0$) that occur at Φ_1 - and Φ_2 -flux, respectively. It corresponds to above-mentioned spectral features at which Eqs. (6), (7) tend to zero. We propose to utilize these features for experimental determination of the SOC strength parameter. As was discussed earlier, up-(down-) steps in

conductance and peak (dip) in thermopower take place at the same chemical potentials. In this sense conductance measurement is equivalent to thermopower measurement for our purposes, and mentioned features can be detected by two methods. Moreover conductance measurements can be simpler and more straightforward from an experimental point of view. The magnitude $\partial G/\partial\mu$ (or $\partial G/\partial V_g$, with V_g being the gate voltage), that is proportional to thermopower in the low-temperature regime in accordance with the so-called Mott formula [20], can be measured directly.

Thus, it is necessary for our purpose to perform the thermopower or conductance measurements in external magnetic field. Specific values of magnetic field, at which the mentioned features occur, can be extracted from a dependence of S or $\partial G/\partial\mu$ on the magnetic field and gate voltage. Inserting these values of magnetic field into Eqs. (6), (7) at $\delta_j^{so} = 0$ and $\delta_j^w = 0$, one will obtain the system of two equations relative to r_0 and α . It is convenient to solve these equations for ground subband $j = -1/2$ (as in Fig. 1b) and using $m^* = 0.026m_0$,

$g^* = -14.9$ for InAs (see for instance Ref. 12). Thus, the numerical solution of equations $\delta_{-1/2}^{so}(\Phi_1) = 0$ and $\delta_{-1/2}^w(\Phi_2) = 0$ gives the values α and r_0 . Although the above system of equations has the high order, but numerical analysis shows the presence of the single nontrivial solution.

V. DISCUSSION AND CONCLUSION

Let us discuss some weaknesses of proposed approach that deal with both experimental problems and flaws of the used simple model.

(i) The proposed approach requires the low temperature thermopower or conductance measurements. We have to compare the temperature not only with character energy scale E_0 but the SO-gap as well in order to one can experimentally discern single peak (dip) in S or $\partial G/\partial \mu$. These measurements have to be performed at temperatures about 1K for the nanowire with $r_0 = 42$ nm ($R = 50$ nm).

(ii) It should be noted that we neglect in our calculation a dependence of the surface 2DEG radius r_0 on the applied magnetic field. At high magnetic field the character length of the radial wave-function localization will be determined by the cyclotron motion, but it does not tend to zero and will be limited by the effective potential of the band bending that prevents the penetration of the wave-function in central area of the nanowire. For the nanowire with $R = 50$ nm ($r_0 = 42$ nm at $B = 0$) [3, 9] the minimal r_0 -value (in the limit $B \rightarrow \infty$) is estimated to be about 30 nm. Our estimations show that at intermediate magnetic field, corresponding to the flux $\Phi \sim \Phi_0/2$ (at such a field $r_0 \sim l_B$ with $l_B = \sqrt{\hbar c/|e|B}$ being the magnetic length; it corresponds to $B \sim 0.35$ T for the nanowire with $R = 50$ nm), r_0 is about 37 nm that differs only by 12 percent from the magnitude of r_0 at $B = 0$. Thus, we hope that our assumption (r_0 does not depend on \mathbf{B}) holds for the proposed α -determination approach in not too strong magnetic field. Nevertheless, in order to obtain more precise estimations it is necessary to solve the consistent problem [9] in magnetic field. However, one should expect, at least, the determined Rashba-parameter to be of the correct order of magnitude in our approach.

One can use a simpler approach: if the surface 2DEG radius is known, e.g. from the consistent scheme [9], then only one equation is necessary. It is convenient to use $\delta_{-1/2}^{so}(\Phi_1) = 0$, because the weaker magnetic field is required for the SO-gap disappearance than for the flat

subband appearance. Moreover, there is no problem of $r_0(B)$ -dependence at weak magnetic fields in this case.

Our approach for SOC strength determination is based on transport detection of SO-gap evanescence in magnetic field. However, for the InAs nanowires the conductance down-steps (SO-gap) were not yet observed comparative to quantum wire defined in 2D structure with high mobility [13]. Nevertheless, we guess that the absence of negative steps in recent conductance quantization experiments [2] deals with no any residual scattering, but it is due to thermal smearing of steps or the absence of W-shape subbands in the energy spectrum due to small effective SOC strength that is proportional to αr_0 . The latter can be due to the small effective radius of surface 2DEG. In this sense, our approach is not applicable for nanowires of small radius.

Recently it was shown [6] that the Rashba-coupling parameter can be tuned in the range $\alpha = 0.5 - 3 \times 10^{-9}$ eV·cm for InAs nanowire that corresponds to dimensionless SOC parameter $\Lambda = 0.15 - 1$ for the nanowire with $r_0 = 42$ nm. Thus, the proposed approach of α -determination is valid in the half of α -tuning interval (we suppose that our approach works adequately at $\Lambda \gtrsim 0.5$).

It would be extremely interesting to compare the results obtained by proposed method and by the standard antilocalization technique [3, 6]. For example, at first one measures Rashba parameter in long wire by the localization-antilocalization, and after that the measurements of SOC parameter are performed by the proposed method in shortened nanowire where ballistic transport takes place.

In conclusion, we have theoretically studied the spectral and transport properties of carriers in InAs nanowire with surface 2DEG in magnetic field. Ballistic conductance and thermopower are shown to have some specific features in dependence on the chemical potential that are due to strong Rashba SOC. These features disappear at certain magnetic fields. The latter allows us to propose the approach for the experimental determination of Rashba-coupling parameter α from thermopower or conductance measurements. Limitations of the proposed approach applicability are discussed.

Acknowledgments

The author is grateful to N.S. Averkiev, P.A. Alekseev, P.V. Petrov and A.Yu. Silov for useful discussions. This work was supported by Russian Ministry of Education and Science (project No. 2665).

-
- [1] S. A. Dayeh, D. P. R. Aplin, X. Zhou, P. K. L. Yu, E. T. Yu, D. Wang, *Small* **3**, 326 (2007).
 - [2] S. Chuang, Q. Gao, R. Kapadia, A. C. Ford, J. Guo, A. Javey, *Nano Lett.* **13**, 555 (2013).

- [3] S. Estévez Hernández, M. Akabori, K. Sladek, C. Volk, S. Alagha, H. Hardtdegen, M. G. Pala, N. Demarina, D. Grützmacher, T. Schäpers, *Phys. Rev. B* **82**, 235303 (2010).

- [4] Y. A. Bychkov, E. A. Rashba, JETP Lett. **39** 78 (1984).
- [5] S. Jin, J. Waugh, T. Matsuura, S. Faniel, H. Wu, T. Koga, Physics Procedia **3**, 1321 (2010).
- [6] D. Liang, X. P. Gao, Nano Lett. **12**, 3263 (2012).
- [7] S. Datta, B. Das, Appl. Phys. Lett. **56**, 665 (1990).
- [8] S. Nadj-Perge, S. M. Frolov, E. P. A. M. Bakkers, L. P. Kouwenhoven, Nature **468**, 1084 (2010).
- [9] A. Bringer, T. Schäpers, Phys. Rev. B **83**, 115305 (2011).
- [10] L. I. Magarill, D. A. Romanov, A. V. Chaplik, JETP Lett. **64**, 460 (1996).
- [11] M. Trushin, J. Schliemann, New J. Phys. **9**, 346 (2007).
- [12] R. Winkler, *Spin-Orbit Coupling Effects in Two-Dimensional Electron and Hole Systems*. (Springer-Verlag, Berlin, 2003).
- [13] C. H. L. Quay, T. L. Hughes, J. A. Sulpizio, L. N. Pfeiffer, K. W. Baldwin, K. W. West, D. Goldhaber-Gordon, R. de Picciotto, Nature Phys. **6**, 336 (2010).
- [14] S. Datta, *Electronic Transport in Mesoscopic Systems*. (Cambridge University Press, Cambridge, 1995).
- [15] C. W. J. Beenakker, H. van Houten, Solid State Phys. **44**, 1 (1991).
- [16] Y. Imry, R. Landauer, Rev. Mod. Phys. **71**, S306 (1999).
- [17] Y. V. Pershin, J. A. Nesteroff, V. Privman, Phys. Rev. B **69**, 121306 (2004).
- [18] P. Streda, J. Phys.: Condens. Matter **1**, 1025 (1989).
- [19] C. R. Proetto, Phys. Rev. B **44**, 9096 (1991).
- [20] M. Cutler, N. F. Mott, Phys. Rev. **181**, 1336 (1969).